Adipose-Tissue-Inspired Viscoelastic Composite for Tunable Soft Implant and Elastomer Applications

Final Report: May 11, 2016

Kyle Kim, Mike Messina, Sadia Naseem, Ian Robinson, Claire Tomaszewski, Casey Vantucci, and Christopher Wong

---

Abstract

Tunable viscoelasticity is highly valuable in biomedical and elastomer applications, with key behaviors such as modulus matching and mechanical damping. By mimicking the structure of adipose tissue, we designed a viscoelastic composite of up to 90% soft cores in shells of stiff matrix. Using Finite Element Analysis and a Voronoi Polyhedron model, we manipulated the viscoelasticities of the core materials, shell thickness, porosity, and cell shape to achieve a broad range of composite properties. Fabrication of a composite utilized emulsion polymerization of PMMA shells around octadecane. Through composite microstructure and composition, we were successful in obtaining composite damping factors from 1 to at least 10 times of the shell damping factor. Although further work must be done to overcome challenges in self-assembly and uncontrolled phase separation in the fabrication, the novel composite microstructure has strong potential to design materials with tailored viscoelasticity.

Motivation

Tunable viscoelasticity is highly valuable in high-performance structural and biomedical applications, as it encompasses both elastic properties such as moduli and strength, as well as time-dependent properties such as mechanical damping and shock resistance (1). Applications of viscoelastic materials include soft medical implants, vibrational damping components in lab instrumentation, engines, machinery, and earthquake resistant structures, shock absorbing parts in sports equipment, and acoustic dampening, which all require specific stiffnesses and damping behavior (2). Currently, materials used for these applications are single phase elastomers or gels, such as rubber and silicone gel. Viscoelastic properties of these elastomers can be altered, albeit in limited fashion, through elastomer chemistry and degree of crosslinking. The development of

a composite with a controlled microstructure and tuned material properties of the individual phases may allow us to achieve a broader range of viscoelastic behaviors than single-phase elastomers can achieve.

Emulating natural structures has been a proven approach to innovation in materials science and engineering. This biomimetic approach has been especially successful in the field of structural materials and biomedical science, where it has played a strong role in the fabrication of honeycomb composites, hollow bone-like scaffolds, biocompatible implants, prosthetics, 3-dimensional cell scaffolds, and anti-fouling surfaces (3). Although much attention has been given to the applications of biomimetic structural materials that are characteristically hard and rigid, less attention has been given to the development of biomimetic materials that exhibit viscoelastic properties (1). Thus, designing and fabricating a soft biomimetic composite is exciting from both the perspective of composites and biomimicry.

One example of a biological soft composite is adipose tissue. Adipose tissue (AT) commonly known as fat tissue, has a variety of essential roles in mammals, including energy and nutrient storage as a fat reservoir (4), thermogenesis, thermal insulation, feedback in metabolic and immune pathways as an endocrine organ (4), and a shock absorber for joints through foot pads and for protection of vital organs (5).

As shown in Figure 1 (4), AT consists of roughly 80-90v/v% liquid triglycerides, which are in the form of fat globules roughly 80μm in diameter each encapsulated by an adipocyte (6).

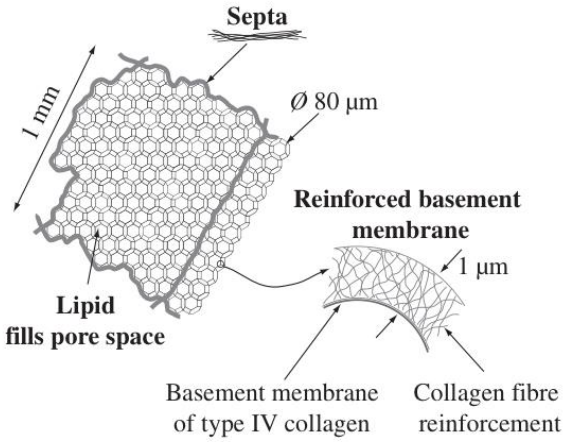

Figure 1: Adipose tissue microstructure (4)

Adipocytes are secured and connected by a collagen-based matrix, known as the basement membrane, with 2μm walls (5). The fat globules act as an incompressible fluid that contributes minimal elasticity, but are essential in preventing the basement membrane collagen network from collapsing (5). Although there are other components of adipose tissue such as thick dispersed collagen fibrils and blood vessels, the basement membrane and adipocytes dictate the bulk mechanical properties of AT (5).

Through the project, we aimed to design and fabricate a composite that mimics the unique microstructure of fat, in particular the basement membrane and adipocytes. The composite will consist primarily of a soft and heavily damping material which be encapsulated within a stiffer shell material during the composite fabrication process. Individual shell-core cells will be sintered together by thermal and/or mechanical processes to form the bulk material. Although adipocytes have liquid cores, we have decided to expand the scope of the composite from a solid-liquid composite to a more general composite using two viscoelastic materials, which may have the potential to achieve a broader range of viscoelastic properties.

Materials Science and Engineering Aspects

In terms of final performance of the composite, the two main engineering aspects of the project are viscoelasticity and mechanical properties of composites. Another major materials science component of project is the synthesis and self-organization of polymers into hierarchical structures, which is challenging from chemistry and phase interface perspectives.

Viscoelasticity, which encompassses time-dependent elastic behaviors, can be considered a sum of elastic and viscous components:

$$E^* = E' + iE''$$

where E* is the complex modulus, E' is the storage modulus (elastic component and ideally equivalent to Young's modulus) and E'' is the loss modulus (viscous component) (2). Viscoelasticity can be measured through a variety of means, most commonly by loading a material sinusoidally and observing the sinusoidal strain response, which will exhibit phase shift, δ, as shown in Figure 2. A phase shift of $\delta = 0$ implies a completely elastic material, while a phase shift of $\delta = \pi/2$ implies a completely viscous material. Incorporating phase shift, the complex modulus can be expressed as: $E^* = |E^*|\cos\delta + i|E^*|\sin\delta$. The loss factor, $\tan\delta$, is equal to E''/E' is the ratio of mechanical energy dissipated to energy stored in cyclic loading, and is a measure of the damping capabilities of the material. In defining tunable viscoelasticity parameters, the two properties we will use in our modeling and analysis are E', which characterizes stiffness of the material in a time-independent scenario, such as a static support, and $\tan\delta$, which characterizes damping capacity (2).

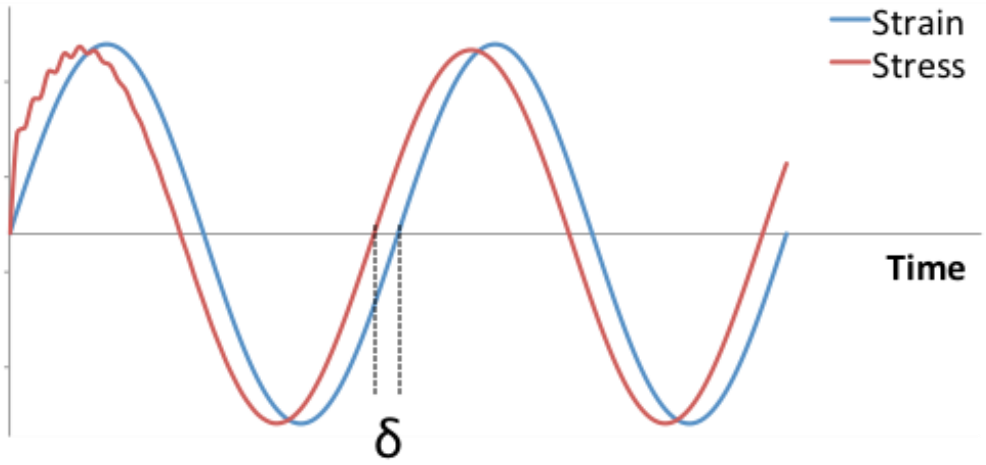

Figure 2: Simulated stress-strain curve time lag curve from one shell-core composite used in FEA modeling

Mechanical properties of composites are a complex function of individual mechanical properties of the individual phases and microstructure of the composite. As the microstructure of the composite determines the load transfer between dissimilar phases, changes in microstructure can drastically change composite properties (6). Many algebraic models for deriving composite material properties from component properties have been developed (7-10). The simplest models, the Voigt and Reuss models, and account for constant-strain and constant-stress cases for composite properties, respectively. The Voigt model represents the upper bound of E' and lower bound of the loss factor, and will be used as a measure of how close or far our composites are from the constant-strain condition (2). In cases of the extreme mechanical properties differences of the two component materials, as may be observed in a solid-liquid composite, the Reuss model gives modulus values of nearly zero, which is not useful for our analysis and will not be used. According to the Voigt model,

$$E'_{composite} = v_s E'_s + v_c E'_c$$

$$tan\delta = \frac{v_s E'_s + v_c E'_c}{v_s E''_s + v_c E''_c}$$

where v is the volume fraction of the various materials (2). However, an input of accurate geometries that more closely resemble our desired composite microstructures is essential in determining more precise viscoelastic properties.

Another mechanical property of the shell-core cells we will explore is the bulk modulus. The bulk modulus, K, defines a material's resistance to isotropic tension or compression, and is given as:

$$K = -V\frac{dP}{dV}$$

where V is the volume of the cell and dP/dV is the gradient of the experimental pressure-volume. Bulk modulus is important especially for applications that experience stresses from a wide variety of directions, and is important in preventing crushing of the foam-like microstructure of the proposed composite (11).

A major sector of materials science and engineering is centered around polymers and biomaterials, which is the main focus of the project. Polymers differ from other materials such as metals and ceramics in that they often do not exhibit crystallinity, making their chemical properties and syntheses much less predictable. Additionally, the rates at which monomers polymerize depends on many factors including concentrations of monomer and initiator, temperature, and radiation flux (for radical polymerizations), all of which can drastically affect the degree of polymerization and polydispersity index of the polymer, in turn affecting the mechanical properties.

For this project, we had to take all of these factors into consideration. The polymerization of poly(methyl methacrylate) around an oil meant that we needed to determine the appropriate reagents and conditions that would allow the polymerization reaction to proceed. Not only must the polymerization reaction occur, but the PMMA must self-assemble around the oil droplets. Self-assembly is a common technique in materials science because it does not require too much hands-on involvement and is solely based on the ways that materials interact. For self-assembled capsules, typically small micelles must first be formed in solution using surfactant, which again depends on factors like surfactant concentration because a critical concentration of surfactant is required to form micelles due to the amphiphilic nature of surfactants as well as shape factors.

In addition to all of the factors that must be considered for polymers in this project, we also have the obstacles associated with biomaterials. In order to form a composite that could be used in the body as an adipose tissue replacement, the material must not adversely interact with the body. Materials engineers extensively investigate how materials interact with the body because they could potentially trigger immune responses, degrade, and develop biofouling, all of which affect the body and also the function of the material itself. For this project, we needed to thoroughly consider the materials we were using in order to determine which would be best in terms of mechanical properties and processability, while also being biocompatible.

Previous Work

The microstructure of adipose tissue is well studied, and will be utilized to design the composite. In addition, the mechanical properties and relation of microstructure to bulk properties of porcine subcutaneous adipose tissue has been studied in detail (6, 12). The material exhibits a characteristic J-shaped stress strain curve, and also shows a nonlinear dependence on strain rate. The elastic moduli of human subcutaneous adipose tissue, human omental adipose tissue, human breast adipose tissue, and decellularized human adipose tissue have been found to have a range of 2-3.5 kPa (6, 12). In addition, the viscoelastic properties of subcutaneous AT have been found to have a loss factor of 0.368 (13). In addition, much of the research surrounding adipose tissue has focused on the biological properties of the tissue and how to use human decellularized adipose tissue as scaffolds for regenerative medicine (14,15). Investigations of the mechanical structure of a variety of adipose tissues have concluded that different types of adipose tissue have a range of mechanical properties; thus, modulus matching is essential in bioimplant applications to prevent disproportionate load transfer to living tissue (12).

To our knowledge, there has been no research attempting to specifically mimic the structure of adipose tissue using a polymer-polymer or polymer-liquid composite. However, disorganized biphasic polymer composites for improved viscoelastic properties are not uncommon. One of the most prominent examples is high-impact polystyrene, which is a copolymer of polystyrene, which is stiff and has poor damping capacity, and butadiene, which forms an elastomeric polymer. The butadiene phase separates during copolymerization, forming unorganized soft phases interspersed in the polystyrene matrix, and improving the impact and damping properties of the polystyrene (16). However, even for super high impact polystyrene and other very highly elastomer-modified polymer, the rubber phase comprises of volume fractions up to 25% v/v, which is far from the up to 90% v/v of lipid cores in adipose tissue (17).

The use of natural and synthetic materials to form capsules containing a liquid or gel is not novel. Much research has been done on these types of capsules with interests for drug delivery, biotechnology, cosmetics, or detergency (18,19). Understanding the properties of the different polymers that can be utilized for bioencapsulation is essential for selecting the proper polymers that can mimic adipose tissue. A comprehensive review on bioencapsulation and characterization of biocapsules critically analyzes the currently used polymers and methods (20).

Some potential methods for encapsulation of a gel-like material include droplet-based microfluidic techniques, encapsulation of oils by phase separation, and emulsification using cross-linking of alginate (21,22,23). Of particular interest is interfacial emulsion polymerization, in which an oil-in-water or water-in-oil emulsion is first formed. Next, the monomer system is added and polymerized, and the polymerized product selectively condenses on the surface of the emulsion droplets due to the relative surface tensions (22). Interfacial emulsion polymerization is useful for creating liquid core microcapsules, and avoids environmental issues due to organic solvent use or dangerous chemicals (22).

Design Goals

Our primary design goals are aimed at successfully mimicking the microstructure of adipose tissue with a biphasic soft composite and tuning the composite properties through changes in material parameters and geometry. The goals fall into two categories: mechanical modeling and fabrication.

In terms of mechanical modeling, we aim to obtain a broad range of elastic and viscoelastic properties from the composite microstructure, in particular E', tan δ, and K. Unlike other structural applications, maximizing or minimizing given viscoelastic properties does not provide the optimal material properties in modulus matching and damping applications; therefore, we do not have specific values of the mechanical properties that we would like to exceed. In addition, as the microstructure is the more novel aspect of the project, we will not specify the exact materials comprising the composite in the mechanical analysis, as the microstructure could be applied to many soft materials, not simply the PMMA and octadecane used in the fabrication. Therefore, resulting values for E', tan δ, and K will be expressed as ratios relative to the shell material. However, reasonable material parameters will also be used in the modeling, in order to explore a reasonable range of properties we can obtain in the composite. Figure 3 shows the range of E and tan δ for known single-phase polymeric materials (25). To simulate a liquid core, a very small E' and K of roughly 1 GPa will be used, which is a common for liquids (26). Actual component material properties may lie slightly outside of the range of values used, so our modeling will provide a moderately conservative estimate of the full range of composite properties.

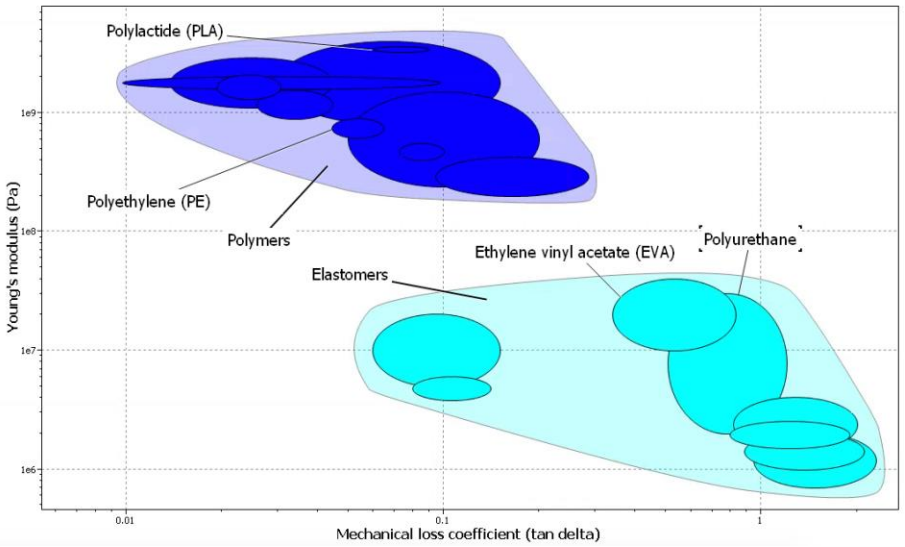

Figure 3: Range of Young's modulus and tan δ for known single-phase polymeric materials (23)

In designing the fabrication process, our goals are to observe the changes in the core mechanical properties through phase-transition from the processes of interfacial emulsion microcapsules, we hope to conduct material characterization in order to refine and improve our modeling design. Consequently, this improved design would allow us to adjust our fabrication methods as well to better mimic the properties of adipose tissue. Furthermore, we hope our methods polymerization and sintering. Through successful fabrication of our PMMA:oil system of fabrication prove to be an effective and viable option for future development of these composites. Ultimately, we expect our design and fabrication processes to have strong potential to create materials with tunable viscoelastic properties.

Technical Approach

In calculating viscoelastic properties of composite materials, we employed two general methods: complex algebraic analysis using a polyhedron composite model and finite element analyses using ANSYS mechanical modeling software. We aimed to obtain consistent viscoelastic properties from both modeling methods to our confidence in developing the composite. Each of the techniques are valuable for the analysis. Algebraic techniques have the advantage of low computational expense which allows acquisition of mechanical properties using a wide variety of input properties; however, they may have limited scope due to inability to change model parameters and failure of the model at extremely limits. Finite element analyses

are much more computationally expensive and thus are difficult to perform on large models using a wide variety of input properties; however, they include fewer model assumptions and more flexibility in controlling model parameters.

Voronoi Polyhedron Modeling

Of the many composite models, we decided to employ the Voronoi polyhedron model for algebraic analyses due to the similarity of the input geometries to the proposed microstructure (10). As shown in Figure 4, the Voronoi polyhedron model captures the cellular, uniform, disorganized, and isotropic structure of microstructure of adipose tissue.

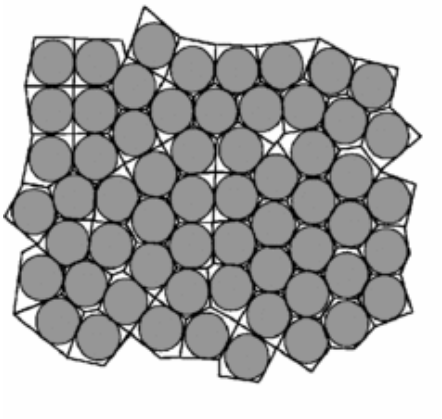

Figure 4: Voronoi polyhedron model of core-shell composite material, with shaded spheres representing core material and lighter areas representing the shell material (10).

The Voronoi model outputs the viscoelastic properties of a core-shell composite material based on the individual viscoelastic properties of both materials that it is composed of and other microstructural geometrical factors. Modifying the Voronoi polyhedron equation slightly to account for the lower complex modulus of the core, the complex modulus of the composite is given as:

$$E^*_{composite} = (1-\pi_1)E^*_s + 2\frac{E^*_s E^*_c}{(E^*_s - E^*_c)^2 \pi_1}\left[|E^*_s - E^*_c|\pi_1 + E^*_c \log_{10}\left(\frac{E^*_c}{E^*_c - |E^*_s - E^*_c|\pi_1}\right)\right];\ \pi_1 = c\left(\frac{3(1-q_v)}{4\pi}\right)^{1/3};\ 1 < c < 2$$

where E^*_c and E^*_s is the complex shear modulus of the filler core and the matrix shell, respectively, c is a shape-dependent constant with c=1 signifying spherical cells and c=2

signifying cube shaped cells, and q_v is the volumetric filler fraction of the core (10). Using a Matlab script to run the Voronoi equation for a variety of core moduli 0.5-0.0001 times the shell modulus of 1.1GPa. In addition, microstructure was manipulated by observing c from 1 to 1.7, and q_v from 0.5-0.95, the loss factor and storage modulus of the composite material were calculated. One of the primary limitations with the Voronoi equation is that when the moduli of the core and shell vary by several orders of magnitude, the equation can lose its validity, and must be compared to the numerical simulations.

Finite Element Analysis Modeling

As the geometry of the composite microstructure was expected to dictate mechanical properties, finite element geometries were carefully selected, aiming to balance conflicting goals of obtaining accuracy and minimizing computational expense. Initial simulations of a square versus a cubic composite cell with equivalent volume ratios and core and shell material properties resulted in the cubic cells having a significant lower modulus and tan δ. This signified that 3D models have additional important modes of load transfer and perform better than 2D models despite the increased expense of the simulation.

We modelled each individual core-shell composite as a single truncated cube cell, as shown in Figure 5. The geometry of the cell was controlled to obtain a fixed core:shell volume ratio, which varied throughout the simulations. To simulate incomplete sintering, a finite porosity between was used and controlled by changing the size of the truncated corners. The E and tan δ of the core and shell materials were individually defined, and the two component materials were connected using bonded contacts were placed between the shell and core. Meshes were automatically generated and for each analysis, each cell comprised over 2000 mesh elements to increase the precision of the analysis and minimize numerical artifacts.

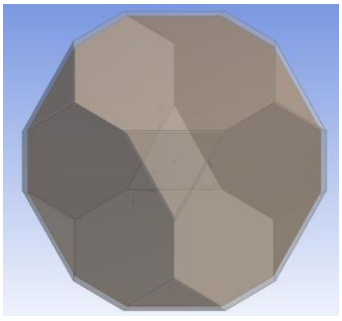

Figure 5: Truncated cube geometry of model shell-core cells used in finite element analysis.

Finite element analyses were performed through the ANSYS modeling software. ANSYS provides adequate built-in and pre-defined mechanical modeling resources for the models. Other than inputting scalar coefficients such as stiffness and damping and defining loads and supports, the finite element models were straightforward. We did not need to change boundary conditions and differential equations governing the mechanical interactions. For all models, simple geometries (cube or square) with one material phase was used to verify the software parameters. Two ANSYS mechanical modules were used to analyze the mechanical properties of the composite material: static structural and transient structural analyses.

Static structural analysis is a simple mechanical testing analysis neglects viscous terms in the viscoelasticity. Although the viscous terms were essential for calculating damping, static structural analysis was appropriate in simulating compression testing for determining bulk modulus. Compressive strains were applied in x, y, and z directions, to approximate hydrostatic pressure. Strains corresponding to volumetric changes of up to 0.5 were used or until the material failed. The bulk modulus was calculated as $K = -VdP/dV$ using the volumetric changes and resulting force reactions. The effect of elastic and bulk modulus of the core and shell materials (including liquid core) were explored using the single truncated cell model for a shell volume fraction of 0.1, shells with Poisson's ratio = 0.4 solid cores with Poisson's ratio=0.4 and bulk moduli of 0.1-0.0001 times the shell, and liquid cores with Poisson's ratio=0.5.

Transient structural analyses comprised the bulk of the composite analyses. Transient structural analysis includes time-dependent behavior, which allowed incorporation of viscoelastic behaviors of the core and shell materials to output damping behavior. Although more computationally expensive, transient structural analysis was used as it allowed input of material-dependent properties while other modules such as modal analysis, did not. Due to the time-dependent nature of transient analysis, solutions at each time point were iteratively solved and thus the analysis is much more computationally expensive than static structural analysis, especially as finite time was required to reach equilibrium behavior. As a result, transient structural analyses could not be performed on very large and complex models, which necessitates constraining the size of and/or simplifying the models.

Transient structural analyses were performed using driven sinusoidal displacements to obtain viscoelastic properties. This simulates dynamic mechanical analysis (DMA), in which the probe provides an oscillating displacement and measures the force required to drive the

oscillation. For our analyses, we chose strain amplitudes of 0.02 with frequencies at 1Hz, which is small enough to prevent large geometrical distortions. Due to time limitations, we were not able to explore the temperature and frequency-dependent of nature of viscoelastic properties and nonlinear elastic effects at large strain amplitudes. As preliminary simulations showed that the force reaction converged within the second cycle of oscillating displacement, the second force reaction cycle was used to determine viscoelastic properties (from t=1 to 2 seconds). We used a time step of 0.02 seconds to provide a reasonable fit of data. Using a linear least square fit, the second force reaction cycle was fit to a sinusoidal curve of 1Hz frequency to determine the phase shift angle, δ, between the displacement and force reaction curves. This was especially necessary for analyzing force reaction curves that were not completely sinusoidal. The effective complex modulus, storage, and loss moduli of the composite was calculated as:

$$E^* = \sigma_{amp}/\varepsilon_{amp}$$
$$E' = E^* cos\delta$$
$$E'' = E^* sin\delta$$

where E* is the magnitude of the complex modulus, E' is the storage modulus, E'' is the loss modulus, σ_{amp} and ε_{amp} are the amplitudes of the reaction stress and of the strain. Ideally, the storage modulus is equivalent to the Young's modulus.

For single truncated cube models, the shell material was set to have a modulus of 1.1GPa, Poisson's ratio of 0.4, and tanδ=0.1, which is reasonable for low-stiffness PMMA (23). As seen in Figure 3, this is a rather conservative estimate for the extremes of the ideally stiff and non-damping shell. In the first set of analyses, the core material was set to have 0.2-0.0001 times the shell modulus, Poisson's ratio of 0.4, and tanδ of 0.5, 1, and 2, which is a good estimate for common elastomers (23). Initial simulations showed that liquid cores showed equivalent viscoelastic properties to low-modulus solids, and therefore were not further investigated. In the second set of analyses, the volume fraction of the shell was changed from 0.1 to 0.5 with core moduli of 0.1 and 0.01times the shell modulus. In the third set of analyses, the porosity of the cells were changed from 0 to 30% with core moduli of 0.1 and 0.01times the shell modulus. Due to the ideally isotropic nature of the proposed composite, changes in direction of applied force were not investigated. Overall, these simulations represented a comprehensive of microstructural and material changes for composite tunability.

Finally to examine the effect of arrays of multiple sintered cells, 2D arrays of up to 20x20

cells or 3D arrays of up to 8x8x8, and the transient structural analyses were obtained in the same manner described above (for 2D arrays, displacements were driven on the largest face). The 3D array ideally modeled the bulk composite most precisely; however, it may not have capture completely isotropic behavior due to the regularity of the octahedron cell arrays. Initial simulations on small 2D and 3D arrays demonstrated that the loss factor did not change regardless of array size or aspect ratio. Therefore, for larger arrays, individual cells were simplified as a single material using the obtained E' from transient analysis, and time-independent static structural analyses were used to determine the effect of array size on the bulk mechanical properties.

Prototype: Materials and Process Selection

The proposed fabrication of the composite prototype occurs in two main steps: synthesis of PMMA shell/octadecane core microcapsules using interfacial emulsion polymerization, and sintering of PMMA shells together in order to form the bulk composite material. The PMMA:oil system was selected based on existing literature on PMMA microencapsulation of long chain alkanes. Advantages of using PMMA include its the biocompatibility and thermoplastic behavior and the low environmental impact of the polymerization process (1, 19-22, 24). We decided on an octadecane core because the oil has a solid-liquid transition temperature of about 30˚C, meaning that we could test the properties of the composite at room temperature, with a solid capsule core, and at body temperature, with a liquid capsule core. This would lead us to utilize the experimental data obtained from the prototype and compare it to the mechanical modeling.

The fabrication for the synthesis of PMMA shell/octadecane core microcapsules using interfacial emulsion polymerization was modified from a method proposed in Sari et al (22). Briefly, we combined deionized water, octadecane, and the surfactant Triton X-100 and mixed for 30 minutes. This mixture was then heated to 40˚C under air (modified from nitrogen) and methylmethacrylate (shell monomer), allyl methyl acrylate (crosslinker), ferrous sulfate, and ammonium persulfate were added. This was mixed for 30 minutes and then sodium thiosulfate and tertbutyl hydroperoxide were added. The final fabrication steps included heating at 90˚C for one hour and then dried in the vacuum oven for 72 hours.

The procedure previously mentioned forms capsules on the order of approximately 200nm in diameter. In order to examine the bulk mechanical properties of individual capsules,

we aimed to additionally form capsules on the order of approximately 1mm that could then be tested in compression. For the larger capsules, deionized water was mixed with octadecane in the absence of surfactant (Triton X-100) in order to prevent the formation of an emulsion and the mixture was heated to 30˚C. Methyl methacrylate, allyl methyl acrylate, ferrous sulfate, and ammonium persulphate were added and stirred vigorously for 30 minutes. The temperature was then raised to 90˚C, sodium thiosulphate and tertbutyl hydroperoxide were added, and the mixture was heated and stirred for one hour before being allowed to rest.

Once the capsules are formed and dried, they must be sintered together to create the adipose tissue-like structure. The capsules are loaded into a hot press and heated to the melting temperature of the PMMA, as determined by differential scanning calorimetry, and pressure is applied to sinter the capsules together into a single, porous structure. The PMMA used for the DSC measurements was formed through the same generalized procedure for the capsules, including the Triton X-100 surfactant but excluding the oil. This allows us to most accurately determine the melting temperature of the PMMA for our capsules, as it will contain additional reagents as well as have a similar degree of polymerization as the PMMA shell of our capsules.

Results and Discussion

Mechanical Modeling

As shown in Figure 6, the bulk modulus of the composite only seemed to depend on the respective bulk moduli of the core materials. This provides a clear advantage of liquid cores to air-filled cores; although neither have any appreciable elastic properties and therefore do not contribute to the composite's storage modulus, the generally high bulk moduli of liquids allow the composite to have good resistance toward compression.

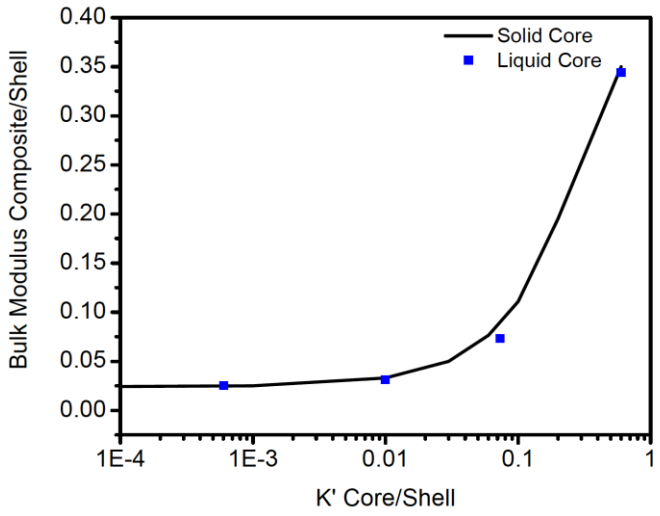

Figure 6: Bulk moduli of composite compared to shell material with respective to solid or liquid nature of core and relative bulk moduli of the core to shell material.

Material parameters for single composites for time-dependent analyses are shown in Table 1 and are generally consistent with polymer and elastomer values (23).

Table 1: Material parameters for shell and core materials used in ANSYS transient analysis

Parameter	Shell	Core
E’	1.1GPa	2.2GPa to 0.11MPa
tanδ	0.1	0.5-2
ν	0.4	0.4

In time-dependent analyses, hysteresis curves of viscoelastic composites were generally near-sinusoidal, with a few high-modulus composites (above E’ core/shell of 0.1) showing some hysteresis distortion at strains of zero (as the stress went from compressive to tensile). Visually, there were no unique morphological events at these distortions, so they were likely due to the bonding contact between the dissimilar core and shell materials as well as insufficient mesh sizing and contact parameters, which led to numerical artifacts arising for the time-dependent nature of the analysis. For lower modulus composites, the sinusoidal fits had low residual sums using least squares regressions, and therefore the viscoelastic properties derived from these simulations should be more accurate.

Viscoelastic behaviors of single cell composites were first investigated. Figure 7 shows the effect of changing the relative E' and loss factors of the core material on the viscoelastic properties of the composite, using a shell volume fraction, pv, of 0.1, and a porosity of 5%. Between E' core to shell ratios of 0.001 and 0.2, there were significant increases in both loss factors and E' of the composite. However, in terms of the core tan δ, there was a large effect of increasing tan δ_{core} on the loss factor of the composite, while there was a much smaller effect on E'. For E' core/shell > 0.01, there were significant differences in loss factor between models with different tan δ_{core}, while differences in E' of the composite were only observed for E' core/shell>1. This suggests that within ranges of 0.01<E' core/shell <0.1, the loss factor of the composite can be highly tuned without significantly affecting the time-dependent elastic properties. Overall, the range of loss factors and E' obtained were 1 to 11 and 0.05 to 0.25 times the shell loss factor and E', respectively. Had a smaller tan δ_{shell} been used, the range of loss factors and E' relative to the shell would be expected to change. Also, the range of E' core/shell range with the composite loss factor and E' having differing dependencies on tan δ_{core} could be altered.

Further, Figure 7 shows that the composites were consistent with the bounds of the Voigt model. At high E' core to shell ratios, the simulated values began to approach the Voigt limit. This suggests that for similar shell and core ratios, the bonding contacts are strong enough to allow nearly perfect load transfer between the shell and core materials, which is reasonable. Another explanation for the approaching limit could be due to the effect of numerical artifacts in hysteresis at high E' core/shell and a resultant non-precise fit; however, as simulated composites even with low values of tan δ_{core} approached the Voigt limit, the effect of numerical artifacts is not expected to be large.

As shown in Figure 8, the effect of the volume fraction of the shell on composite viscoelasticity was significant, with increasing shell thickness and the volume fraction of the shell decreasing the loss factor and increasing E' of the composite, as expected. By manipulating the shell thickness from 0.1 to 0.5, loss factors decreased by up to 3 times, which was more prominent for the high E' core/shell ratio model. Similarly to the effect observed in Figure 7, for low shell thicknesses, the loss factor and E' approached the Voigt limits. This can be explained as there is greater contact surface area to volume ratio of the shell for thinner shells, which would improve load transfer.

Figure 9 shows the effects of porosity on the viscoelastic properties of the composite by increasing the dimensions of the truncated cube corners. Even with relatively large porosities of 30%, there appeared to be only a slight increase in loss factor, while there was a large decrease in E' of the composite. This suggests that incomplete sintering of the microcapsules may be beneficial in tuning the modulus of the composite while not affecting loss factor much. Overall, the effect of porosity had the least influence on viscoelasticity when compared to core material viscoelastic properties and shell thickness.

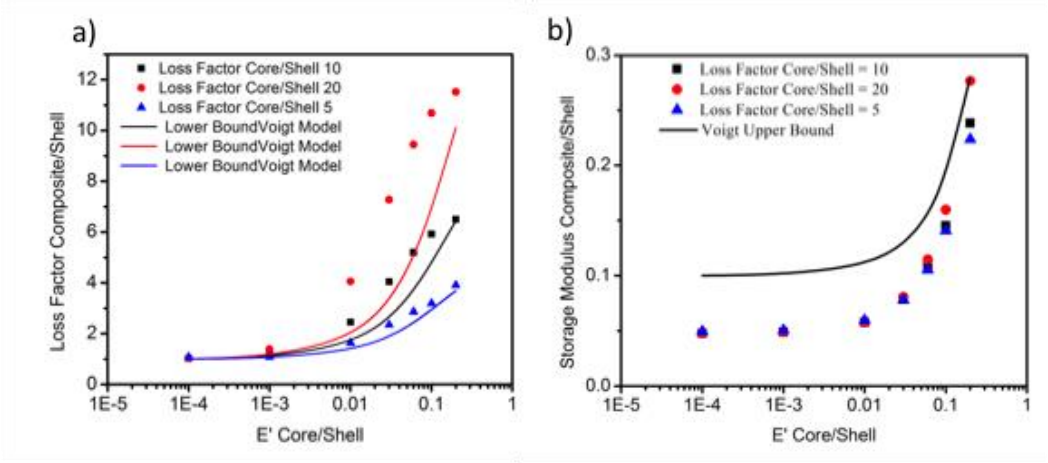

Figure 7: Effect of loss factor and E' of core material on a) loss factor and b) E' of the single cell composite in finite element analysis in ANSYS transient analysis software. Shell-volume fractions were set at 0.1, tan δ_{shell} was 0.1, porosity was 10%.

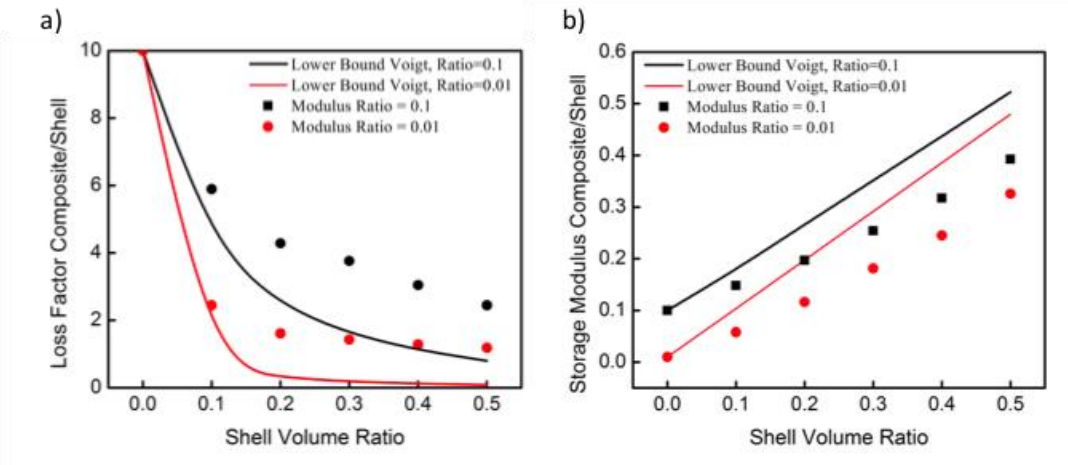

Figure 8: Effect of shell volume ratio on a) loss factor and b) E' of the single cell composite of the single cell composite in finite element analysis in ANSYS transient analysis software. E' core/shell were set at 0.1 and 0.01, tan δ_{shell} was 0.1, and porosity was 10%.

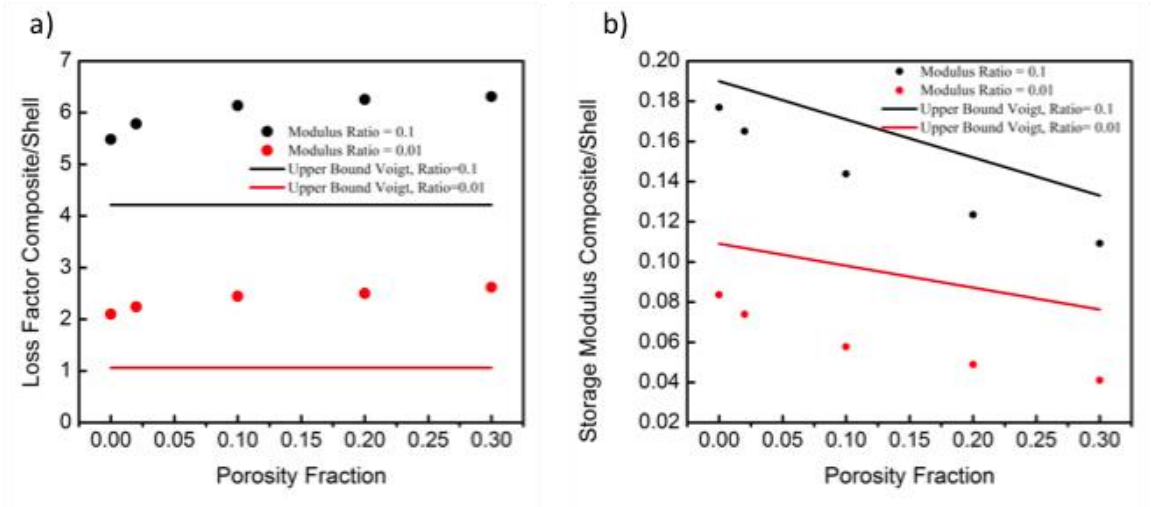

Figure 9: Effect of porosity fraction on a) loss factor and b) E' of the single cell composite of the single cell composite in finite element analysis in ANSYS transient analysis software .E' core/shell were set at 0.1 and 0.01, tan δ_{shell} was 0.1, and shell volume fraction was 0.1.

The effect of cell arrays was investigated for composites with E' core/shell of 0.1, shell volume fractions of 0.1, tan δ_{shell} of 0.1, and porosity of 10%. As shown in Figure 10, E' increased for the flat 2D array of cells but began to level off at very high cell numbers (20x20). The increase in apparent E' suggests that the shape factor and aspect ratio of the bulk material may be an essential in controlling the effective stiffness of parts created with the composite. However, for the 3D array of cells, the modulus remained the same as the single octahedron, suggesting that single octahedrons are generally sufficient for calculating the viscoelastic properties of the composite, unless the bulk material has very high aspect ratios.

Although potentially having a significant effect on the viscoelastic of the composite, the direction of applied forces were not considered in our analysis. This was because the final composites we aim to synthesize will not have long range order, with the core-shell cells resembling an amorphous structure. The 2D and 3D arrays were stacked regularly, which could have potentially increased the load transfer between the core-shell cells and increased the apparent moduli, but without complex, random Voronoi polyhedron models of the composite microstructure, it is difficult to determine the effects of array regularity.

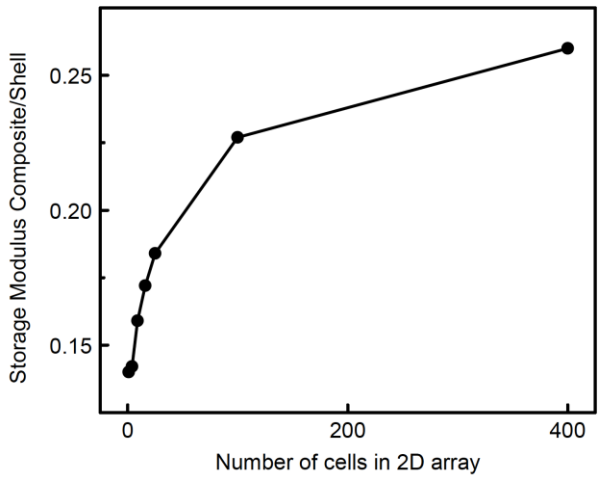

Figure 10: Effect of 2D array size on E' of the single cell composite of the single cell composite in finite element analysis in ANSYS transient analysis software .E' core/shell were set at 0.1 and 0.01, tan δ_{shell} was 0.1, and shell volume fraction was 0.1.

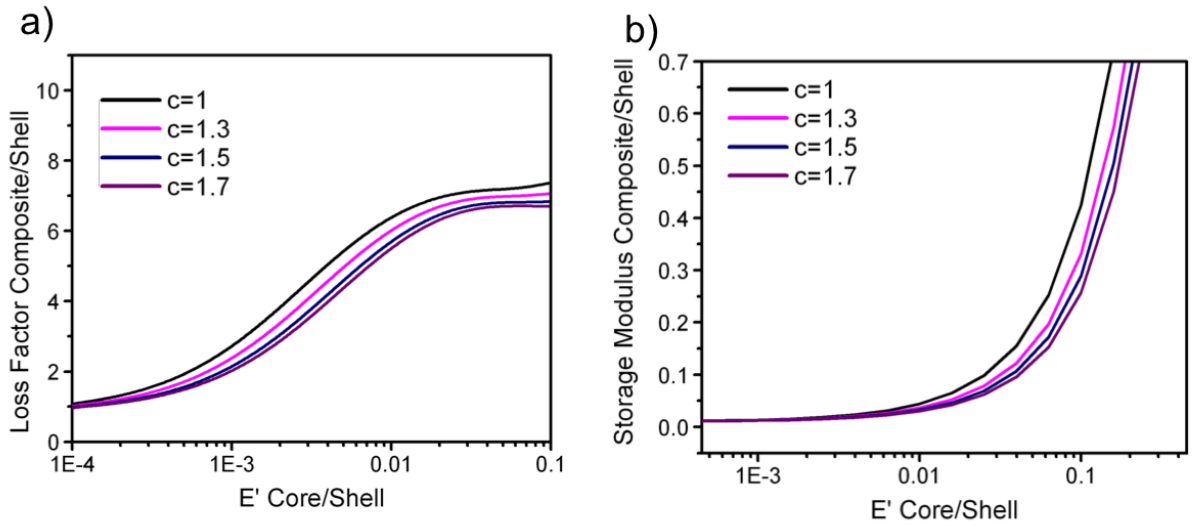

Figure 11: Using Voronoi polyhedron model, effect of ratio of E' to core and shell and c-shape factor. a) loss factor and b) E' of the soft composite. E' core/shell were set at 0.1, tan δ_{shell} was 0.1 ,tan δ_{shell} was 1 and shell volume fraction was 0.1.

As shown in Figure 11, the Voronoi polyhedron model effectively modeled the mechanical properties of the composite material based on varying shape and composition parameters. Figure 11A represents the effect of shape factor on the loss factor of the composite material, which increased with the E' core/shell property until a plateau around a value of E' core/shell=0.03. Figure 11B shows a sharp increase in the storage modulus composite/shell as the value of E' core/shell increased. The shape-dependent constant c was varied from 1,

representing a spherical composite, to 1.7, representing a shape similar to a truncated cube. As the shape tended towards spherical, higher values were observed for both loss factor and storage modulus; however, this was a rather minor effect.

Although not shown in Figure 11, the calculated composite E' exceeded the upper bound for the Voigt model, which calls into question the accuracy of the model at high E' core/shell ratios. From a geometrical standpoint, there are a variety of reasons why the Voronoi model may have not been completely accurate. The limitations of the models include that the model assumes that the cores are spherical, which will not be the case for the compressed and sintered composite, that the core has a larger complex modulus than the shell, and that there was no porosity and no degrees of freedom in terms of how the Voronoi polyhedron were bonded together (10). Therefore, due to not meeting these assumptions, the results of viscoelastic from the Voronoi equation were not as reliable.

Comparing the Voronoi polyhedron model to the finite element analysis in Figure 7, the shapes for the loss factor and E' curves with respect to core/shell modulus were similar, but were shifted toward lower values of E' core/shell. In addition, the characteristic region where the composite loss factor was sensitive to changes in E' core/shell, while the composite was not similarly shifted. This shift implies that the Voronoi model accounts for much lower load transfer between the shell and core materials in the cell. Although not completely in agreement, the Voronoi polyhedron model helps confirm the FEA models as the shapes were similar, but suggests that the Voronoi polyhedron model was less accurate than the FEA models, especially as they contradicted the Voigt limits at high E' core/shell.

Prototype Fabrication

Overall, the process for fabricating our prototype was successful. Using the procedure written by Sari et al, we were able to successfully encapsulate octadecane in a PMMA shell to form capsules on the order of approximately 100μm. However, we were unable to encapsulate the oil on the scale of 1mm, and therefore we were not able to test the mechanical properties of our capsules to verify our models. We were also successful in synthesizing empty PMMA capsules to be used for thermal property analysis for the sintering process.

For the first experiment, we followed Sari's procedure, with the previously mentioned modifications, for the 200nm capsules (22). The result was observed under the microscope, as shown below in Figure 12.

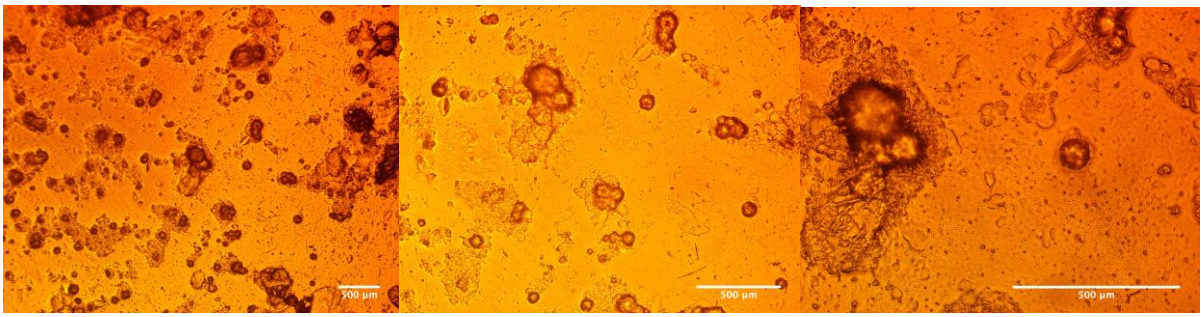

Figure 12: Images from the original fabrication method of the pre-dried microcapsules at 10x (left), 20x (middle), and 40x (right) . The scale bars in all three images represent 500µm.

Based on our synthesis method and as seen in the figure above, we were able to achieve microcapsules with a PMMA shell and an octadecane core; however, the microcapsules did not have a narrow size distribution, which was not incorporated in the analysis. Further, we aimed to create microcapsules of ≈100µm diameter in order to mimic the AT, but the microcapsules were smaller than desired. Although the reaction forces of the bulk material during mechanical analyses are independent of individual cell size, a certain microcapsule size is required for characterization using the rheometer. The microcapsules were analyzed using ImageJ to determine the core size, shell size, overall size, and core to shell ratio. These average values are shown below in Table 2.

Table 2: Characterization of Microcapsules from Initial Fabrication Method

	Core size (um)	Core + Shell (um)	Shell size (um)	Core to Shell ratio
AVG	60.98	103.30	39.83	1.624
STDEV	32.64	34.91	10.70	0.794

From Table 2, it can be seen that there are extremely large standard deviations for the sizes of the microcapsules, signifying non-uniform synthesis. Further, the core to shell ratio was around 2:1, which is significantly different from the core to shell ratio used in the modeling

stages. Therefore, further modifications on the synthesis method must be made to achieve uniform, larger microcapsules at a higher core to shell ratio.

The second set of experiments attempted to fabricate larger capsules to be used for mechanical compression testing in the rheometer. To achieve larger capsules, surfactant was excluded from the reaction to prevent the formation of an emulsion, resulting in larger oil droplets around which the PMMA would polymerize. For the first attempt, the mixture separated into three phases: aqueous, organic, and solid. This was likely due to the lack of stirring while the mixture cooled, allowing the oil to form a layer on the surface of the water and the PMMA to polymerize in the aqueous phase and then settle to the bottom of the vial.

Subsequent attempts were made to form the larger capsules, but none were successful. With constant vigorous stirring, the PMMA never crosslinked, the reason for which is unclear. Additionally, we tried using more crosslinker, initiator, and monomer, and also attempted to initiate polymerization with brief exposure to ultraviolet light. The lack of polymerization could be due to many different factors. Since we were using chemicals donated by Professor Raghavan, some of the chemicals could have expired or been contaminated, affecting their polymerization. Self-assembly of polymers and capsules is often highly dependent on hydrophobicity, and surfactants create the interface that allows materials to interact for assembly in aqueous environments. It is also possible that by excluding the surfactant from the synthesis, there was no surface on the oil to which the PMMA could adhere and polymerize.

As mentioned, we also needed to fabricate capsules consisting of a PMMA shell without the octadecane core to be used for DSC measurements. We were successful in doing so, and were able to produce a white PMMA powder. Initial testing of the PMMA revealed that it was too crosslinked to determine the melting temperature using the DSC. However, the high degree of crosslinking was due to an experimental error and the PMMA that is actually encapsulating the oil for the composite is less crosslinked. Unfortunately, due to time constraints and scheduling conflicts, we were unable to re-test our PMMA shells and therefore could not obtain a melting temperature to be used for the sintering process.

Mimicking the functions of adipose tissue such as heat production or energy storage could be a great stepping stone for advancements in many different fields. The tunable properties from these composites would allow for a broad range of uses across many fields. The technology from this project could be translated to structural and mechanical designs, which would alter the

environmental and ethical impacts. Both ethically and environmentally, biodegradability and biocompatibility would be less of a concern. Because of the wide variety of applications a polymer composite with tunable properties can have, some of the ethical and environmental implications can be challenging to predict, so that is also a concern.

Broader Impacts

A soft material with tunable viscoelastic properties offers immense of potential uses for *in vitro, in vivo,* and commercial applications. A successful design will result in a synthetic material that mimics properties of adipose cells and adipose tissue constructs at both the microscale and macroscale. It has been shown that a designed biomimetic material can be utilized as an advantageous scaffold for tissue engineering. A polymeric material can be altered in order to create an adjustable scaffold that promotes tissue growth and regeneration through physical properties such as biodegradability, stiffness, and porosity (16). Additionally, a successful, biocompatible material can be further altered as a method for targeted drug release. Polymers that have the ability to respond to external stimuli can greatly increase the efficacy of medicines in an *in vivo* environment (12). The ideal material result of this design project would present biocompatible materials that would allow for use both *in vitro* and *in vivo*.

Along with medical applications, the tunable viscoelastic properties and control of time-dependent properties such as mechanical damping and shock absorbance have translations to instrumentation, machinery, sports, and medicine. For example, the structure of adipose tissue leads to its protective, cushioning properties that can be mimicked with the synthetic material presented here. A successful material could then be utilized to protect damaged organs or joints in surgical applications. The ability to create a polymer composite that mimics the physical properties of adipose tissue presents the opportunity to replace currently used rubbers and gels with a tunable solid-liquid composite that has a multitude of applications ranging from structural to medical.

Intellectual Merit

The proposed soft composite represents a novel class of tunable structural materials. The physical separation between the nearly elastic and viscous components in forms of polymer shell and elastomer or liquid core on the micro-scale may provide increased control of and expand the

range of viscoelastic properties for a variety of applications. In contrast, in most viscoelastic materials such as elastomers and gels, the viscoelastic properties are derived from contrasting molecular structures within a single phase: cross-linked portions of the phase provides elastic properties, while amorphous sections of polymer or solvent provide viscous components (25). Furthermore, the viscoelastic properties of these materials are modified via chemical means such as cross-linking, functionalization, co-polymerization, etc. (25). Unfortunately, chemical modification does not give a range of mechanical properties for a given material, and modification strategies are limited by the chemical nature of the viscoelastic materials. By using a two-phase composite, we aim to overcome limitations of chemical modification and provide a method to control viscoelastic properties over a broad range.

In addition, the proposed biomimetic composite has intellectual merit as a structural material, as it is essentially a closed foam with an incompressible core. Foam materials are generally filled with air, which is highly compressible and does not resist cell collapse under increased pressures. Incompressible cell cores theoretically improve resistance to cell collapse due to a high bulk modulus and prevention of cell wall buckling (6). Further, in some designs of the composite, the proposed core material is a liquid. Therefore, solid-liquid composites would have increased novelty as their liquid cores would have no definite shape and thus would not form residual interfacial stresses or delaminate. As interfacial stresses or defects rapidly deteriorate material properties, a solid-liquid composite could have increased lifetime and fatigue resistance. Within the field of composites, failures often originate in poor interfaces between component phases, which make the elimination of hard phase boundaries especially attractive (2).

In terms of composite fabrication, the proposed soft composites' fabrication method also uses unique bottom-up approach. As the microcapsules are formed via a self-assembled interfacial emulsion polymerization, the fabrication process can be well studied and controlled before scale-up. In addition, the sintering process is novel as it bridges the gap between microfabrication and macroscale parts, which balances the high control of the bottom-up microencapsulation approach with the scalable processing properties of bulk materials.

Ethics and Environmental Impact

The ethical issues for this project are relatively low, large implications for the advancement of soft material technologies. The main ethical and environmental concerns lie in the materials selection and fabrication of the microcapsule-based composite. In general, capsule syntheses are compatible with non-hazardous materials and has been widely used in medicine (20, 21). However, in terms of materials selection, many materials for encapsulation could pose environmental risk with respect to disposal, such as synthetic plastics or certain oil cores. Especially in large scale syntheses of the proposed composite as high performance materials applicable in all industries, the low environmental risk of the materials are paramount. In addition, the fabrication of composite could pose other ethical concerns, due to hazards in chemical synthesis such as the use of large quantities of solvent and initiator, scale up may prove challenging. Microscale syntheses are often energy and chemically intensive, which pose a concern as to the energy costs and environmental impacts of scaled up production of the material (2).

Additional ethical concerns are application based. If the biomimetic composites were to be used in biomedical applications such as cosmetic surgery or implants, one of the largest factors to consider would be biocompatibility and biodegradability. Existing materials have already been developed for biocompatibility, but these materials would need to be compatibilized for the synthesis process. In applications that withstand significant weathering, the composite must have sufficient degradation resistance and not leach harmful components into the surrounding environment. However, for many general applications, such as vibrational damping for machinery, many of these ethical considerations are not present.

Conclusions

Mechanical modeling of the soft cellular composite demonstrated their strong potential for developing materials with tunable viscoelasticities. Using high bulk modulus core materials, the composite was shown to have a large bulk modulus regardless of value of Young's modulus, demonstrating the advantage of using liquid cores over unfilled foams. Through time-dependent FEA and the Voronoi polyhedron model, broad ranges of viscoelastic properties, with loss factors exceeding 10 times the loss factor of the stiff matrix. The ratio of core E' to shell E', loss

factor of the core material, shell thickness, porosity, and shape factor of the cells all had considerable effects on the overall viscoelasticity of the composites.

A successful prototype was not developed due to complications in synthesis of the PMMA-oil microcapsules, which resulted in microcapsules with low encapsulation efficiency, irregular shapes, and thick shells. Despite changes in surfactant concentrations, reaction conditions, and crosslinker concentrations, we encountered and were not able to overcome challenges in uniform self-assembly of the PMMA shells around the oil cores during the polymerization process. This led to inability to create the final prototype as there were few core-shell cells available to be sintered together into the bulk material.

Future Work

Due to unanticipated complications of the capsule synthesis, further work is needed for the design of the adipose-tissue-inspired composite. Although we were able to successfully encapsulate octadecane in PMMA, an efficient method for separating the capsules from PMMA sheets developed in side reactions must be developed. In addition, we must overcome the high polydispersity of capsule morphologies, which is undesirable for sintering and uniformity of the composite. These complications may be solved by using a different polymerization method, such as radical polymerization using UV, or the use of a different initiator such as benzoyl peroxide. Additionally, alternative polymers and microencapsulation processes could be used to create stiffer or more flexible composites based on their viscoelasticities.

Once uniform microcapsules are produced, we would be able to test and optimize their sintering properties to not only control the composition, but porosity and c-shape factor of the composite. Finally, we would then be able to test the viscoelastic properties of the fabricated composite material, and determine the accuracy of FEA and geometrical models based on the material parameters of the PMMA shell and oil core, which we would obtain separately. For specific applications, the composite would need to be further tested in terms of degradation properties and biocompatibility.

In terms of modeling, many more time-dependent analyses beyond viscoelasticity should be explored, which are beyond the scope of this project. Firstly, high-strain deformations could be investigated to explore nonlinearities in elasticity, a property seen in many biological composites, including adipose tissue. Secondly, impact and shock properties could be explored,

which are limits of viscoelasticity at high strain rates and are indicated in fracture and failure. Thirdly, fatigue properties of the composite microstructure could be determined, which is especially important due to the large interfacial boundaries between the core and shell materials. Before its use in high performance applications, the mechanical properties of the adipose-tissue-inspired composite must be well understood and developed to its full potential.

Acknowledgements

We would like to acknowledge Dr. Raymond Phaneuf for his support and guidance throughout the duration of this project. We would also like to acknowledge the University of Maryland Department of Materials Science and Engineering for funding. Further, we would like to acknowledge both Dr. Srini Raghavan and Dr. Peter Kofinas for providing us with materials, instrumentation, and access to their laboratories.

References

1. Jang, Kyung-In, et al. "Soft network composite materials with deterministic and bio-inspired designs." *Nature Communications* 6 (2015).
2. Chawla, Krishan K. *Composite materials: science and engineering*. Springer Science & Business Media, 2012.
3. Shin, Sera, et al. "Bio-Inspired Extreme Wetting Surfaces for Biomedical Applications." *Materials* 9.2 (2016): 116. Print.
4. Kershaw, Erin E., and Jeffrey S. Flier. "Adipose tissue as an endocrine organ." *The Journal of Clinical Endocrinology & Metabolism* 89.6 (2004): 2548-2556.3.
5. Cannon, Barbara, and J. A. N. Nedergaard. "Brown adipose tissue: function and physiological significance." *Physiological Reviews* 84.1 (2004): 277-359.
6. Comley, Kerstyn, and Norman A. Fleck. "A micromechanical model for the Young's modulus of adipose tissue." *International Journal of Solids and Structures.* 2010, 47(21): 2982-2990.
7. Kim, H. et al. "On the rule of mixtures for predicting the mechanical properties of composites with homogeneously distributed soft and hard particles." *Journal of Materials Processing Technology*. 2001, 112(1): 109-113.
8. Barbero, E. J., and R. Luciano. "Micromechanical formulas for the relaxation tensor of linear viscoelastic composites with transversely isotropic fibers."*International Journal of Solids and Structures* 32.13 (1995): 1859-1872.
9. Hashin, Z. (1965). Viscoelastic behavior of heterogeneous media. J. Appl. Mech., Trans. ASME, 32E, 630-636.
10. Novikov, V.V. and Friedrich, C, "Viscoelastic properties of composite materials with random structures." *Physical Review E*. 2005, 72: 02156.
11. Callister, William D. *Fundamentals Of Materials Science And Engineering*. Hoboken, NJ: John Wiley & Sons, 2005. Print.
12. Omidi, E. et al. "Characterization and assessment of hyperelastic and elastic properties of decellularized human adipose tissues." *Journal of Biomechanics*. 2014, 47(15): 3657-3663.
13. Geerligs, Marion, et al. "Linear viscoelastic behavior of subcutaneous adipose tissue." *Biorheology* 45.6 (2008): 677-688.

14. Yu, C. et al. “Porous decellularized adipose tissue foams for soft tissue regeneration.” *Biomaterials*. 2013, 34(13): 3290-3302.
15. Wu, I. et al. “An Injectable Adipose Matrix for Soft-Tissue Reconstruction.” *Plastic and Reconstructive Surgery*. 2012, 129(6): 1247-1257.
16. Katime, Issa, JoséR Quintana, and Colin Price. "Influence of the microstructural morphology on the mechanical properties of high-impact polystyrene." *Materials Letters* 22.5 (1995): 297-301.
17. Alfarraj, Abdulrahman, and E. Bruce Nauman. "Super HIPS: improved high impact polystyrene with two sources of rubber particles." *Polymer* 45.25 (2004): 8435-8442.
18. Alkhouli, N et al. “The mechanical properties of human adipose tissues and their relationships to the structure and composition of the extracellular matrix.” *American Journal of Physiology-Endocrinology and Metabolism*. 2013, 305(12): E1427-E1435.
19. Sukhorukov, G. et al. “Intelligent micro- and nanocapsules.” *Progress in Polymer Science.* 2005, 30(8-9): 885-897.
20. Malmsten, M. “Soft drug delivery systems.” *Soft Matter*. 2006, 2(9): 760-769.
21. De Vos, P. et al. “Multiscale requirements for bioencapsulation in medicine and biotechnology.” *Biomaterials*. 30(13): 2559-2570.
22. Sari, Ahmet, et al. "Microencapsulated n-octacosane as phase change material for thermal energy storage." *Solar Energy* 83.10 (2009): 1757-1763.
23. Parris, N. et al. “Encapsulation of essential oils in zein nanospherical particles. *Journal of Agricultural and Food Chemistry.* 2005, 53(12): 4788-4792.
24. CES EduPack software, Granta Design Limited, Cambridge,. UK, 2009.
25. Cengel, Yunus A. *Fluid mechanics*. Tata McGraw-Hill Education, 2010.
26. Ratner, Buddy D., et al. *Biomaterials science: an introduction to materials in medicine*. Academic press, 2004.